18th Brazilian Congress of Thermal Sciences and Engineering
November 16–20, 2020 (Online)

ENC-2020-0311
Influence of turbine rotor diameter on the cost of energy of utility-scale wind farms

Michel Ituji Kumimoto
Jhoseny Souza Santos
William Corrêa Radünz
Laboratório de Engenharia de Processos de Conversão e Tecnologia de Energia, Universidade Federal de Santa Catarina, Trindade, Florianópolis - SC, 88040-900.
michel.ituji@gmail.com, jhosenysantoss@gmail.com, w.radunz@posgrad.ufsc.br

Júlio César Passos
Universidade Federal de Santa Catarina, Departamento de Engenharia Mecânica, Bloco A3, 3ºAndar, Trindade, Florianópolis - SC, 88040-900.
julio.passos@lepten.ufsc.br

Abstract. *The improvement of technologies in the area of materials, the project of components, and computational simulations have been making possible the increase of both the wind turbines' rotors size and its lifetime, with estimations going from 20 years to 25 years already. Furthermore, the advances in the wind farms projects have been evolving and allowing to increase the number of layout options as a consequence. Looking forward to finding out the advantages of choosing a larger rotor diameter, it was obtained data from two Greek wind farms located on complex terrain, both with the same wind turbines manufacturer and power (Gamesa 2 MW), but with different diameters: site A with 12 turbines and 90 m of rotor diameter, and site B with 8 wind turbines and 114 m of rotor diameter. Therefore, the swept area of one single wind turbine from site B is 60 % larger than from the site A. Furthermore, in order to obtain the wind map, roughness, and power densities in the study area and estimate the annual production of the wind farms, MERRA-2 wind reanalysis data were used together with information of topography, local vegetation, layout and model of the wind turbines. The results show the capacity factor, from both wind farms A and B, of 0.4 and 0.5, respectively, even though site B has a nominal power of 16 MW and mean wind speed of 7.6 m/s and the corresponding values from site A are 24 MW and 8.1 m/s. Therefore, it concludes that the choice of bigger wind turbines, together with the technological advances on the project of blades and new wind farms layouts, results in a reduction of the cost of energy.*

Keywords: *Renewable energy, Wind, Rotor diameter, Capacity factor, Complex terrain.*

1. INTRODUCTION

The electric power industry is directly related to the development of a country, once it becomes necessary to supply both the industrial demand and population growth. Therefore, there are high expectations for initiatives on the renewable energy field, having a close approach to the sustainable development topic. In this context, wind energy studies have been constantly improving as a result of several decades of scientific research and technological development. Nonetheless, it is also known that there are still grand research challenges. The topic of the increasing size of wind turbines and its variables appears on one of those challenges, mentioned by VEERS *et al.* (2019) as the aerodynamics, structural dynamics, and offshore wind hydrodynamics of enlarged wind turbines: "for both land-based and offshore applications, the industry is seeking even larger turbines that access higher wind speeds aloft and provide further economies of scale, reducing manufacturing, installation, and operational costs per unit of plant capacity".

As a consequence of continuous developments in wind power generation, more options were made possible for investors on projects. There are studies in this way that looks forward to finding out how the project variables work together, improving the understanding of the phenomena at the same time it can bring, for example, increasing cost-effectiveness by influencing decision making and consequently increase the attractiveness on renewable wind energy.

Using a mesoscale numerical prediction model known as Weather Research and Forecasting (WRF), LEE *et al.* (2019) showed interest in analyzing the optimal hub height of a wind turbine that minimizes the cost of energy in for places with distinct geographical characteristics, all over South Korea. In this study, the annual energy production was calculated for increments of height, so the cost curve could be calculated and minimized, afterwards, the rotor diameter was analyzed by compensating the energy loss from a general height of reference. Therefore, as both annual energy production and rotor diameter increase, the size of the turbine is determined. de SÁ (2015) calculated the annual energy production, the capacity factor, and investigated which variables influence the generation of a wind farm in the Northeast region of Brazil. It is presented new layout options based on simulations on Wind Atlas Analysis and Application Program (WAsP), aiming for the ones that can have the same or higher annual production using a minor number of wind turbines. One of the options was found out to be possible to have the same wind farm rated power reducing from 32 wind turbines with 42 m of rotor diameter to only 10 with 90 m of rotor diameter, distancing 4 rotor diameters from each other. Both studies show how the layout variables influence the final generation output, such as hub height, size of the rotor, and rated power. To achieve a complete perspective, de SÁ (2015) suggests for future studies, to analyze the economic characteristics of the new layout options to find the one that minimizes the costs.

Similarly, CHOURPOULIADIS *et al.* (2012) used wind data collected by two meteorological masts to make a preliminary investigation of the future installation of two different wind farms in Greece, comparing the energy production, noise emission, and also a brief financial assessment applying two methods: one based on WAsP, and the other on Computer Fluid Dynamics (CFD). Although the two wind farms are located on complex terrain and use the Vestas V-80 2MW model with 78 m of hub height, both are situated in distinct regions (Western and Northern) and have a different number of wind turbines (13 and 42)

Concerning the wind turbine optimization problem, FUGLSANG *et al.* (2002) detailed the process to approach the minimum cost of energy for different types of wind farms (distinct terrain and wind behavior). For each wind farm, it was considered different scenarios, one of them included the variation of the rotor diameter and tower design. For complex terrain, where the loads on the turbines were high, it was mentioned that as a consequence of the manufacturers' design, the reduction in the cost of energy was very limited. Also looking forward to minimizing the generation costs, McKENNA *et al.* (2015) used mean wind speed data together with different models of wind turbines to estimate the cost-potential in Europe by allocating them from a database to specific sites.

Knowing that there are gaps in the economic topic in the wind energy sector, this work focuses on analyzing the energy production of two wind power plants projects, both located on the Aetolia-Acarnania region, West regional unit of Greece. Wind farm A has 12 turbines and 90 m of rotor diameter, and wind farm B has 8 wind turbines and 114 m of rotor diameter. Therefore, the swept area of one single wind turbine from wind farm B is 60% larger than from the wind farm A. In 2017, Siemens-Gamesa was the company responsible for the wind turbines (G90-2MW and G114-2MW) on both projects. It is noticeable some characteristics between the projects (SIEMENS-GAMESA, 2017):

- Both are on the same geographical region, having a distance around 40 km from each other;
- The turbines are located over complex terrain near the coast;
- Both models have 2 MW of rated power;
- Rotor diameters are 90 m (12 turbines) and 114 m (8 turbines);

A previous study by BAGIORGAS *et al.* (2008) estimated the wind power densities at four selected sites in the central area of Western Greece. It was concluded that coastal regions might be suitable for wind power utilization, while the inland locations are inappropriate. Therefore, it turns out to be interesting analyzing how both projects are compared to each other, having a closer look at the total installed power and production, as well as the influences of the rotor size over the production and how costs are affected by choosing larger turbines. In this context, this work looks forward to searching, at first, for wind resources on the interest geographical region, so it can be possible to study the wind potential. Afterward, simulate on WAsP both layouts, estimate annual energy production, calculate the capacity factor and, finally, make an economic analysis. A better understanding of the project is expected after all the data is processed.

2. METHODOLOGY

2.1 TOPOGRAPHY AND ROUGHNESS MAP

The wind farms (in the polygons), in Fig. 1, are located on a complex terrain near the Mediterranean Sea. Thus, terrain effects must be considered on the wind behavior. The terrain data was obtained from NASA's Earth Observing System Data and Information System (EOSDIS), having a spatial resolution of 1 arc-second (about 30 m)(SRTM, 2015). So, it was possible to process the terrain elevation contour curves and determine the roughness of the wind farms in the nearby area. Google Earth Pro software was used to delimit the areas associated with different roughness types and Global Mapper to process the curves altogether. The values for each roughness type was based on a surface terrain-cover database available in WAsP (MORTENSEN *et al.*, 2014), taking into account the typical Mediterranean vegetation and plantation areas. The final map is then generated using the WAsP map editor tool. Naming the wind farms as site A (the eastern one) and site B (the western one), the Fig. 2 shows how it was done for site B.

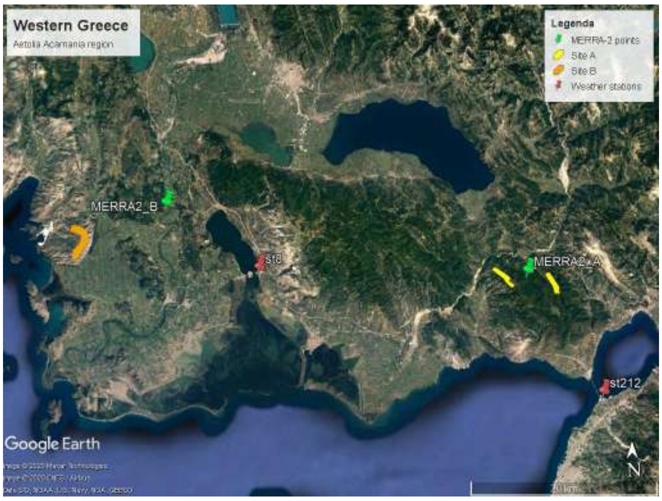

Figure 1. Aetolia Acarnania region(Google Earth, 2020)

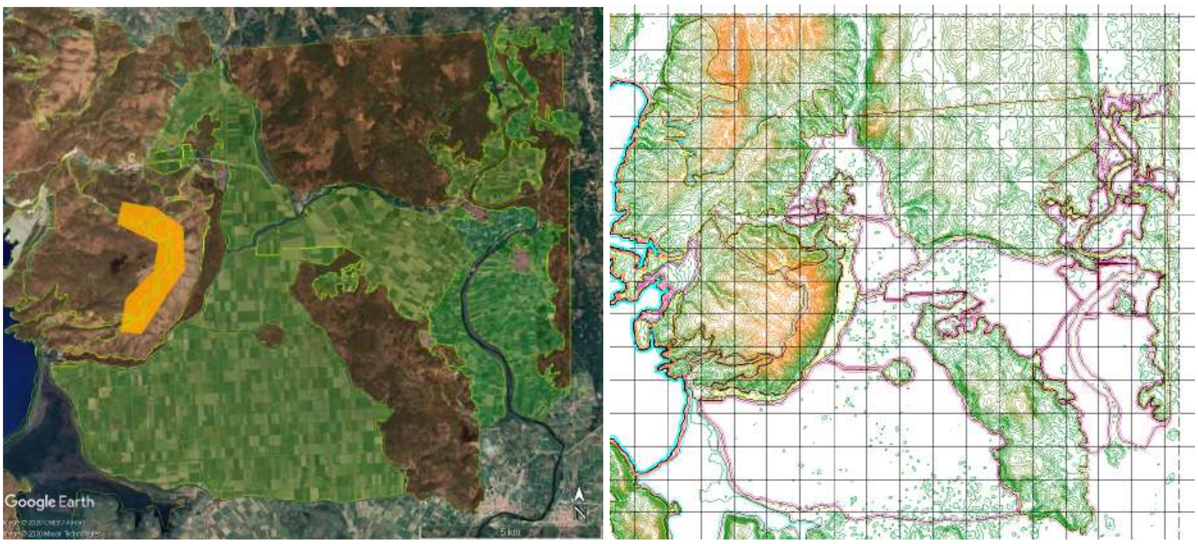

Figure 2. Site B roughness areas (on the left) and final map (on the right)

2.2 Wind farms project data

The exact layout for both wind farms as well as the turbines information was obtained from government transparency portals and is shown in Fig. 3 and Fig. 4. More detailed data from the wind turbines, showed in Tab. 1, were obtained from manufacturers' catalogs.

2.3 Wind energy potential

In order to estimate the wind energy potential near the area of interest, wind data such as horizontal wind speed and direction from at least one year were necessary. Considering that observational data at the site's location was not openly available, another alternative was taken. Since Weather Research and Forecasting (WRF) and Computer Fluid Dynamics (CFD) models demand large computational resources to run, MERRA-2 (Modern Era Retrospective-Analysis for Research and Applications) reanalysis data were chosen for this work. MERRA-2 is a global assimilation system(GELARO *et al.*, 2017), from which the horizontal wind speeds may be obtained, as shown in Tab. 2.

The coarse spatial resolution of the aforementioned data required the usage of interpolation within the wind farms to obtain the wind speeds near the site A. The interpolation used was a spline type which requires four data grid points in the same dimension and is based on the cubic type interpolation. For site B, the original MERRA-2 grid point was around 9 km close to the wind farm, so none interpolation was necessary. To create the wind atlas for the region using the WAsP Wind Climate Analyst tool, the orography and roughness maps and MERRA-2 wind data were used altogether.

Figure 3. Site A Layout

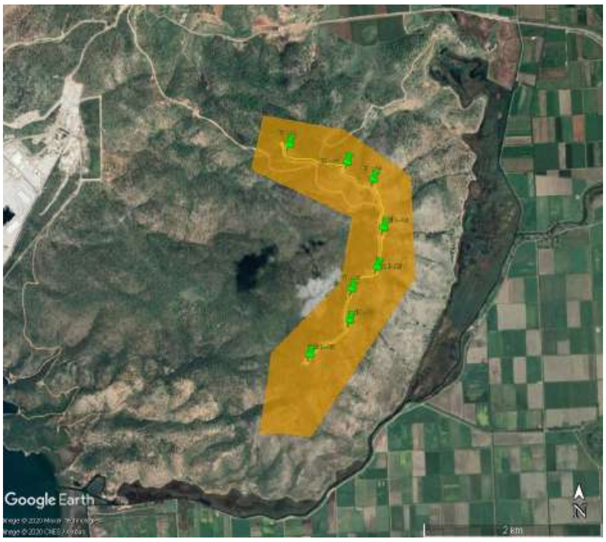

Figure 4. Site B Layout

2.4 Simulation

To make the analysis possible, some variables need to be calculated. Placing all the turbines according to the respective wind farm original project arrangement, together with the power curve and coefficients (thrust and power) into the simulation, the net Annual Energy Production (AEP) can be obtained. Therefore, the Capacity Factor (CF), which is the ratio of the actual delivered power to the theoretical maximum possible, can be calculated using Eq. (1). (ZHANG, 2015)

$$C.F = \frac{Actual\ Power\ Production}{Rated\ Power\ Running\ Full\ Time} \times 100\% \tag{1}$$

2.5 Economic analysis

The economic analysis and intercomparison between the two wind farms required the estimation of certain parameters since the real budgets of these projects are not openly available. To reduce the number of variables, and consequently, the source of errors, two metrics were employed. The first one is an estimation of the individual turbine cost, and the second one is the net AEP. The estimated cost of the turbines was provided by the marketing sector of Siemens-Gamesa, and it was also mentioned that values may vary from one project to another. Considering the proximity between both wind farms and the terrain similarities, it was assumed in this work that costs related to transportation and installation should not vary. For site A (G90-2MW model) the estimated cost is $1,610,000$€, and for site B (G114-2MW model) it is $1,840,000$€.

Table 1. Wind Farms Information

	Site A	**Site B**
Number of Turbines	12	8
Rated Power	2 MW	2 MW
Hub Height	78 m	93 m
Rotor Diameter	90 m	114 m
Total Installed Power	24 MW	16 MW
Total Swept Area	76341 m^2	81656 m^2

Table 2. MERRA-2 wind data characteristics

Size of the Mesh (Lat. x Lon.)	5 x 6 [degrees]
Latitude Resolution	0.5 [degrees]
Longitude Resolution	0.625 [degrees]
Altitude	50 [m]
Time Resolution	1 [hour]
Data Interval	2017-01-01 to 2018-12-31

Therefore, the individual cost of energy (in €/MWh) is obtained as follows:

$$Individual\ Cost\ of\ Energy = \frac{Estimated\ Turbine\ Cost}{Mean\ Annual\ Energy\ Production} \tag{2}$$

2.6 Wind data analysis

Due to the use of the reanalysis data and its interpolation, a reference is necessary to evaluate the results. Once observational data of the meteorological towers at the sites were not available, values from the national weather stations database (LAGOUVARDOS *et al.*, 2017) in the region were used to make comparisons. The closest five weather stations were chosen to be analyzed, the information about each one is shown in the Tab. 3. Also, considering that the instruments are near to the ground level, a vertical extrapolation was necessary, thus the logarithm law equation (Eq. 3) was used for this (HAU, 2004). Their respective roughness, used in the vertical extrapolation, was chosen according to the surroundings.

$$\overline{v}_H = \overline{v}_{ref} . \frac{\ln \frac{H}{z_0}}{\ln \frac{H_{ref}}{z_0}} \tag{3}$$

Where:
$\overline{v}_H$ = mean wind velocity at elevation H (m/s)
$\overline{v}_{ref}$ = mean wind speed at reference elevation H_{ref} (m/s)
H = height (m)
H_{ref} = reference elevation (measuring elevation) (m)
$\ln$ = natural logarithm

Table 3. Weather Stations Information

Station	Altitude	Instrument's Height	Roughness at the site
st7	72m	2m	0.8m
st8	3m	4m	0.4m
st173	902m	2.5m	0.8m
st212	2m	5m	0.6m
st320	55m	4m	0.8m

Afterward, the MERRA-2 data was used again to make interpolations at the weather stations site. This way, it was made possible to compare the interpolation values and the observational data from the stations. The objective was to apply the method that was used at the wind farms site: firstly, MERRA-2 wind data followed by a horizontal wind speed interpolation, concluding with a vertical wind speed extrapolation. The data from all the weather stations are in the same time series as the simulation (2017-01-01 to 2018-12-31).

2.7 RESULTS AND DISCUSSION

From the simulation, a wind atlas for the studied area was obtained with a horizontal resolution of $110m$. The mean wind speed and power densities values at the location of the turbines, and the shape Weibull parameter (Weibull-k) at the MERRA-2 grid point (considered as a meteorological mast) for both wind farms are in Tab. 4. The Weibull-k parameter is directly related to the wind behavior, meaning that for higher Weibull-k values the wind is unlikely to suffer from wide variations. Using a different time series (2003-2005), BAGIORGAS *et al.* (2008) calculated an average Weibull-k parameter of 1.44 at a location close to the weather station $st8$.

Table 4. Wind resource results

	Site A	Site B
Mean wind speed (Turbine site) [m/s]	8.14	7.57
Mean power density (Turbine site) [W/m^2]	810	610
Weibull-k (MERRA-2 site)	1.74	1.74

For sites A and B, the map of power densities and wind speed are in Fig. 5 and Fig. 6 respectively. It can be noticed that the turbines are sited over areas of enhanced wind resources because of the flow acceleration on tops of hills and ridges. The net and gross annual energy production, the proportional wake losses results simulated using WAsP, and the calculated capacity factor for site A and site B are shown in Tab. 5. Site A noticeably produces more power than site B because of the higher number of wind turbines.

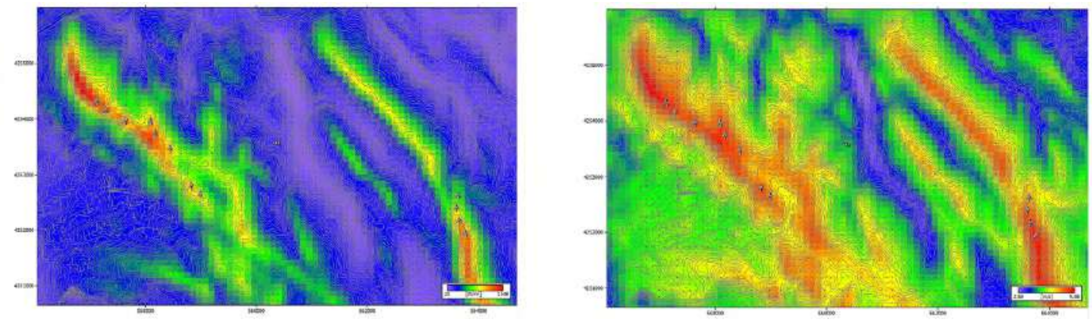

Figure 5. Site A power density map (left) and wind speed map (right)

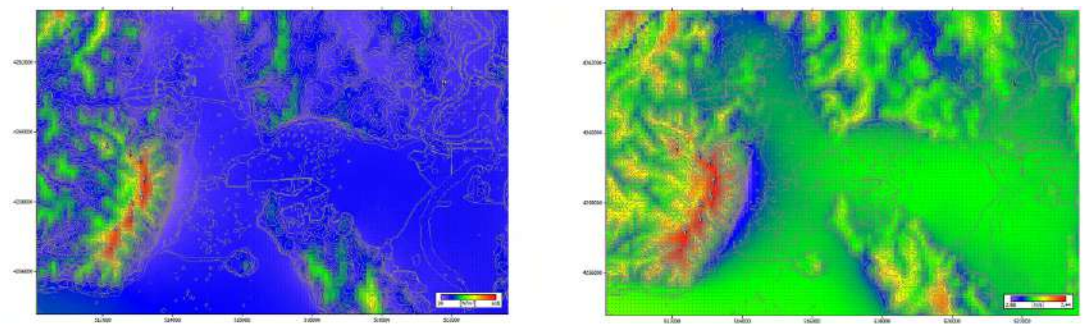

Figure 6. Site B power density map (left) and wind speed map (right)

The calculated individual cost values, from Eq.2, and the mean net energy production of one mean wind turbine from site A and site B are in Tab. 6. The cost is usually associated to a project lifetime estimated to be 20 years, taking this into account, an average wind turbine is estimated to produce 20 times its mean net AEP value through the lifetime period, resulting in $144,540[MWh]$ and $174,280[MWh]$ for site A and B, respectively. The values applied in the Individual Cost of Energy estimation considered only the wind turbine, not to ignore that there are other projects associated costs. Therefore, the real cost of energy should be higher than the one reported here.

The data from the two closest stations (st212 to site A and st8 to site B), in Fig. 7, were used to calculate the difference between MERRA-2 interpolated wind speed and its mean value. After analyzing the time series from both stations, it can

Table 5. Generation results

	Site A	Site B
Total gross AEP [MWh]	87,496	71,571
Total net AEP [MWh]	86,728	69,713
Proportional wake loss [%]	0.9	2.6
Capacity Factor [%]	41.2	49.7

Table 6. Individual Costs Results

Turbine	Estimated turbine cost [€]	Mean net AEP [MWh]	Individual Cost of Energy [€/MWh]
G90-2MW (Site A)	1,610,000	7,227	222.78
G114-2MW (Site B)	1,840,000	8,714	211.15

be noticed that even though there is an abrupt increase in March of 2018 at st212 and a sudden decline in November of 2018 at st8, the values maintain a seasonal behavior oscillating over its mean within an interval of four months.

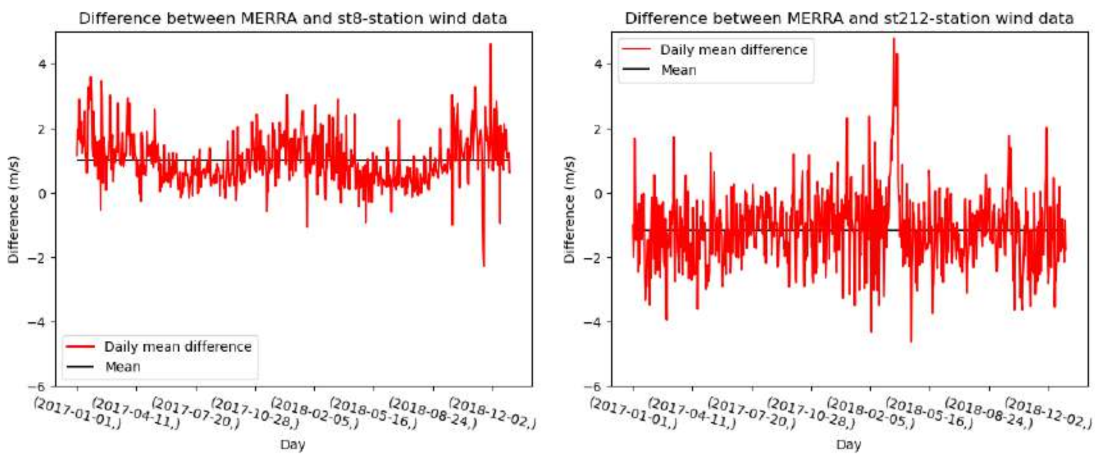

Figure 7. Comparison between wind data

3. CONCLUSION

As expected, the capacity factor for site B is higher than site A (same values were found for an individual mean turbine on both wind farms). This was based on the fact that increasing the rotor diameter, the turbine can extract more power from the air. Analyzing the mean speed values, site B has higher values than site A, which is coherent with the choice of the turbine model (the power curve is moved slightly to the left), being able to be more productive even in low-speed conditions. This higher production can be explained by the fact that the power varies with the cube of the wind speed. It was observed that there are more proportional wake losses from site B, which has larger turbines. That can be justified once the wake area behind the wind turbines becomes larger.

Comparing the calculated Individual Cost of Energy, there is a reduction of 5% from a mean wind turbine from site B to site A. In other words, the higher cost was compensated by the higher production of the larger turbine (site B). These results are based on a MERRA-2 spatial resolution, followed by horizontal and vertical extrapolations that can lead to values different from reality. It is also known that WAsP simulation has limitations in complex terrain. To make more realistic comparisons related to both energy production and cost evaluation, observational wind data from a meteorological mast at the wind farms location are necessary to have as an input parameter on WAsP, the same way it is necessary installation costs values, the annual recurring costs of operations and maintenance, which can vary depending on the conditions of the wind farm layout (terrain complexity, nearby roads, availability and others).

4. ACKNOWLEDGEMENTS

This work was made possible with the support of CNPq (Conselho Nacional de Desenvolvimento Científico e Tecnológico - Brasil).

5. REFERENCES

BAGIORGAS, H.S., Mihalakakou, G. and Matthopoulos, D., 2008. "A statistical analysis of wind speed distributions in the area of Western Greece". *International Journal of Green Energy*, Vol. 5, No. 1-2, pp. 120–137. ISSN 15435075. doi:10.1080/15435070701839488.

CHOURPOULIADIS, C., Ioannou, E., Koras, A. and Kalfas, A.I., 2012. "Comparative study of the power production and noise emissions impact from two wind farms". *Energy Conversion and Management*, Vol. 60, pp. 233–242. ISSN 01968904. doi:10.1016/j.enconman.2012.01.024. URL `http://dx.doi.org/10.1016/j.enconman.2012.01.024`.

de SÁ, F.I.P., 2015. *Efeito da esteira de aerogeradores sobre a produção do parque eólico de beberibe*. Master's thesis, Universidade Federal de Santa Catarina, Florianópolis, Brasil. doi:10.1017/CBO9781107415324.004.

FUGLSANG, P., Bak, C., Schepers, J.G., Bulder, B., Cockerill, T.T., Claiden, P., Olesen, A. and van Rossen, R., 2002. "Site-specific Design Optimization of Wind Turbines". *Wind Energy*, Vol. 5, No. 4, pp. 261–279. ISSN 1095-4244. doi:10.1002/we.61.

GELARO, R., McCarty, W., Suárez, M.J., Todling, R., Molod, A., Takacs, L., Randles, C.A., Darmenov, A., Bosilovich, M.G., Reichle, R., Wargan, K., Coy, L., Cullather, R., Draper, C., Akella, S., Buchard, V., Conaty, A., da Silva, A.M., Gu, W., Kim, G.K., Koster, R., Lucchesi, R., Merkova, D., Nielsen, J.E., Partyka, G., Pawson, S., Putman, W., Rienecker, M., Schubert, S.D., Sienkiewicz, M. and Zhao, B., 2017. "The modern-era retrospective analysis for research and applications, version 2 (MERRA-2)". *Journal of Climate*, Vol. 30, No. 14, pp. 5419–5454. ISSN 08948755. doi:10.1175/JCLI-D-16-0758.1.

HAU, E., 2004. *WIND TURBINES - Fundamentals, Technologies, Application, Economics (2nd ed.)*, Vol. 2. ISBN 0849382246. doi:10.1036/0071425799.

LAGOUVARDOS, K., Kotroni, V., Bezes, A., Koletsis, I., Kopania, T., Lykoudis, S., Mazarakis, N., Papagiannaki, K. and Vougioukas, S., 2017. "The automatic weather stations NOANN network of the National Observatory of Athens: operation and database". *Geoscience Data Journal*, Vol. 4, No. 1, pp. 4–16. ISSN 20496060. doi:10.1002/gdj3.44.

LEE, Kim, Kang and Kim, 2019. "Determining the Optimized Hub Height of Wind Turbine Using the Wind Resource Map of South Korea". *Energies*, Vol. 12, No. 15, p. 2949. doi:10.3390/en12152949.

McKENNA, R., Hollnaicher, S., Ostman, P. and Fichtner, W., 2015. "Cost-potentials for large onshore wind turbines in Europe". *Energy*, Vol. 83, pp. 217–229. ISSN 03605442. doi:10.1016/j.energy.2015.02.016. URL `http://dx.doi.org/10.1016/j.energy.2015.02.016`.

MORTENSEN, N.G., Heathfield, D.N., Rathmann, O. and Nielsen, M., 2014. "Wind Atlas Analysis and Application Program: WAsP 11 Help Facility".

SIEMENS-GAMESA, 2017. "Siemens gamesa delivers wind turbines for three projects in greece with a total capacity of 60 mw". Siemens Gamesa. 22 Nov. 2017 <https://www.siemensgamesa.com/newsroom/2017/11/siemens-gamesa-delivers-wind-turbines-for-three-projects-in-greece-with-a-total-capacity-of-60-mw>.

SRTM, 2015. "The Shuttle Radar Topography Mission (SRTM) Collection User Guide". pp. 1–17. URL `https://lpdaac.usgs.gov/documents/179/SRTM_User_Guide_V3.pdf`.

VEERS, P., Dykes, K., Lantz, E., Barth, S., Bottasso, C.L., Carlson, O., Clifton, A., Green, J., Green, P., Holttinen, H., Laird, D., Lehtomäki, V., Lundquist, J.K., Manwell, J., Marquis, M., Meneveau, C., Moriarty, P., Munduate, X., Muskulus, M., Naughton, J., Pao, L., Paquette, J., Peinke, J., Robertson, A., Rodrigo, J.S., Sempreviva, A.M., Smith, J.C., Tuohy, A. and Wiser, R., 2019. "Grand challenges in the science of wind energy". *Science*, Vol. 366, No. 6464. ISSN 10959203. doi:10.1126/science.aau2027.

ZHANG, M.H., 2015. *WIND RESOURCE ASSESSMENT AND MICRO-SITING*.

6. RESPONSIBILITY NOTICE

The authors are solely responsible for the printed material included in this paper.